INTERNATIONAL JOURNAL OF
NUMERICAL ANALYSIS AND MODELING
Volume 2, Supp , Pages 1–14

BAROCLINIC MATHEMATICAL MODELING OF FRESH WATER PLUMES IN THE INTERACTION RIVER-SEA

HERMILO RAMÍREZ LEÓN, HÉCTOR ALFONSO BARRIOS PIÑA, CLEMENTE RODRÍGUEZ CUEVAS, AND CARLOS COUDER CASTAÑEDA

Abstract. The estuarine zone is an area of strong interaction between fresh and salty water. Dynamics in these areas is complex due to the interaction of the forcing mechanisms such as wind, tides, local coastal currents and river discharges. The difference of density between fresh water and salted water causes the formation of the buoyant plumes which have been investigated by means of numerical models and field studies. Plumes play a significant role in the transport of pollutants and the ecology in the frontal areas where density gradients are strong. Therefore, in order to investigate the horizontal and vertical dispersion of salinity and temperature the YAXUM/3D baroclinic numerical model was developed. The model is validated and applied for two particular cases. The first one consist of modeling the discharge of a jet of hot water where the gradients of temperature prevail and the second to study the discharge of the mouth of the estuary Leschenault toward the Koombana bay, Australia where salinity gradients are analyzed. The results derived from the YAXUM/3D are satisfactory and in agreement to with other models which have been already validated.

Key Words. estuarine zone, baroclinic modeling, buoyant plume, vertical mixing.

1. Introduction

The estuarine zone is a complex area due to the interaction of wind, tides, local coastal currents and river discharges. In this area, the fresh water moves toward the sea on top of the salty water layer. The dynamics of the frontal area play an important role in the biology of the area due to the accumulation of particulate organic matter. In addition, the daily heating and cooling effect produce changes of temperature in both rivers and marine waters [1].

In coastal areas, the interaction of fresh water river discharges into the sea causes the formation of the buoyant plumes. In order to investigate de dynamics of buoyant plumes laboratory, field measurements and numerical simulations have been carried out thoroughly. Also, a significant ecological impact has been observed due to amount of particles and pollutants brought along with the river flow.

Numerical models have proven to be a successful tool to investigate buoyant plumes. So different environmental conditions can be simulated in relatively short periods of time. Oceanographers have established different approaches to classify their own models. One of the most important approaches in the literature is the

Received by the editors December 22, 2005.
2000 *Mathematics Subject Classification.* 35R35, 49J40, 60G40.

consideration of the density variation, where the models are classified as barotropic or baroclinics. Although this approach is derived from the oceanic classification models, it is wise to take it into account in what refers to applications in estuaries, outlets or coastal lagoons, because in some cases, important processes exist due to the change of densities.

The difference between a barotropic and baroclinic models resides in the vertical discretization and on the determination of the pressure term in the Reynolds equations. In the barotropic models the vertical integration is applied and therefore, density is uniform with depth, while in the baroclinic models vertical process are considered such as gradients of temperature, salinity and density.

In this paper, a baroclinic numerical model is developed and validated for buoyant fresh water plumes discharging to the coastal environment. In the first part, the numerical model is described and in the second part the validation and applications examples are showed. The results are compared to those derived by McGuirk and Rodi [2]. In the second application a dispersion of fresh water plume into a marine environment is modeled. Basically, attention is paid to the simulation of the salinity behavior. In this case we are reproducing the work developed by Okely [3], who works with another numerical model whose application was given for the Koombana Bay in Australia.

2. The Numerical Model

The YAXUM/3D numerical model was developed and solves the three dimensional equations for a free surface flows based on the numerical scheme proposed by Casulli and Cheng[4], where the numerical solution is given by a combination of a semi-implicit Eulerian-Lagrangian numerical scheme.

2.0.1. Governing equations. These equations describe the velocity fields and the free surface variations. The density is solved by means of a state equation in function of a temperature, salinity and pressure fields. The model solves a salinity and temperature transport equations. For the pressure two kinds of approximations are taken in account. The first one is the hydrostatic approach where the pressure P changes with the depth (z), according to

$$\frac{\partial P}{\partial z} = -\rho g \tag{1}$$

This relation is valid if the horizontal dimension is larger than the vertical one, which is the main consideration for the shallow water equations approach.

The second consideration is named the Boussinesq approximation, where density may be considered as a constant in all terms, except the gravitational term.

Horizontal velocities:

$$\frac{\partial \overline{U}}{\partial t} + \overline{U}\frac{\partial \overline{U}}{\partial x} + \overline{V}\frac{\partial \overline{U}}{\partial y} + \overline{W}\frac{\partial \overline{U}}{\partial z} = -\frac{1}{\rho_0}\frac{\partial \overline{P}}{\partial x} - \frac{\partial \overline{u'u'}}{\partial x} - \frac{\partial \overline{u'v'}}{\partial y} - \frac{\partial \overline{u'w'}}{\partial z} + f\overline{V} \tag{2}$$

$$\frac{\partial \overline{V}}{\partial t} + \overline{U}\frac{\partial \overline{V}}{\partial x} + \overline{V}\frac{\partial \overline{V}}{\partial y} + \overline{W}\frac{\partial \overline{V}}{\partial z} = -\frac{1}{\rho_0}\frac{\partial \overline{P}}{\partial y} - \frac{\partial \overline{v'u'}}{\partial x} - \frac{\partial \overline{v'v'}}{\partial y} - \frac{\partial \overline{v'w'}}{\partial z} - f\overline{U} \tag{3}$$

Vertical velocity:

$$\frac{\partial \overline{W}}{\partial z} = -\left(\frac{\partial \overline{U}}{\partial x} + \frac{\partial \overline{V}}{\partial y}\right) \tag{4}$$

Free surface equation:

$$\frac{\partial \overline{\eta}}{\partial t} = -\frac{\partial}{\partial x}\left(\int_{-d}^{\eta} \overline{U} dz\right) - \frac{\partial}{\partial y}\left(\int_{-d}^{\eta} \overline{V} dz\right) \tag{5}$$

Temperature equation:

$$\frac{\partial \overline{T}}{\partial t} + \overline{U}\frac{\partial \overline{T}}{\partial x} + \overline{V}\frac{\partial \overline{T}}{\partial y} + \overline{W}\frac{\partial \overline{T}}{\partial z} = \frac{\partial}{\partial x}\left(K_{Tx}\frac{\partial \overline{T}}{\partial x}\right) + \frac{\partial}{\partial y}\left(K_{Ty}\frac{\partial \overline{T}}{\partial y}\right) + \frac{\partial}{\partial z}\left(K_{Tz}\frac{\partial \overline{T}}{\partial z}\right) \tag{6}$$

Salinity equation:

$$\frac{\partial \overline{S}}{\partial t} + \overline{U}\frac{\partial \overline{S}}{\partial x} + \overline{V}\frac{\partial \overline{S}}{\partial y} + \overline{W}\frac{\partial \overline{S}}{\partial z} = \frac{\partial}{\partial x}\left(K_{Sx}\frac{\partial \overline{S}}{\partial x}\right) + \frac{\partial}{\partial y}\left(K_{Sy}\frac{\partial \overline{S}}{\partial y}\right) + \frac{\partial}{\partial z}\left(K_{Sz}\frac{\partial \overline{S}}{\partial z}\right) \tag{7}$$

Density equation[5]:

$$\rho\left(\overline{S}, \overline{T}, \overline{P}\right) = \frac{\rho_0}{\left(1 - \frac{\overline{P}}{k_P}\right)} \tag{8}$$

where ρ_0 is the reference density and k$_P$ is a constant coefficient. These values and the formulation (8) are obtained from UNESCO[6].

Therefore, hydrodynamic is described by a four variables ($\overline{U}, \overline{V}, \overline{W}$ and $\overline{\eta}$) given by equations (2),(3),(4) and (5). For the thermodynamic, temperature, salinity and density are given by equations (6),(7) and (8). Pressure P from the state equation (8) is the hydrostatic pressure and can be computed at any time.

2.0.2. Numerical solution. The model solves the equations with the two options of a vertical integrated or multilayer model. A staggered grid cell is used where the vectorial variables are evaluates in center of each face and the scalar at the center of cell (Figure 1)

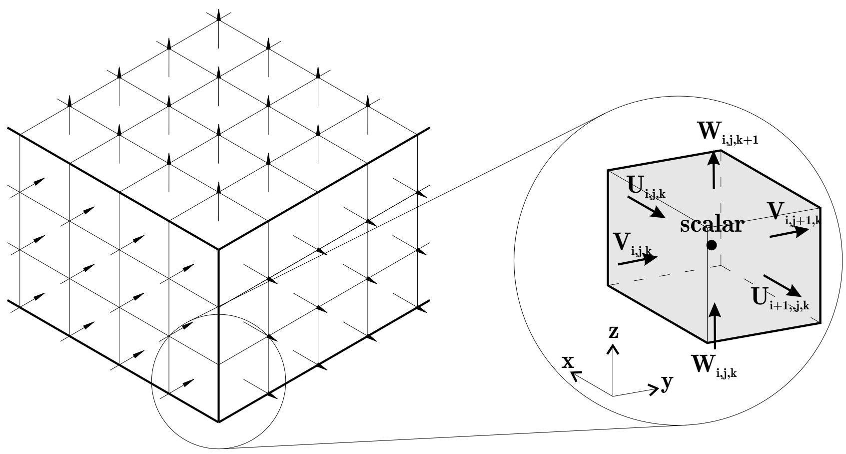

FIGURE 1. Variables position on the numerical cells

The vertical grid can be defined as uniform or variable vertical layers as shown in Figure 2.

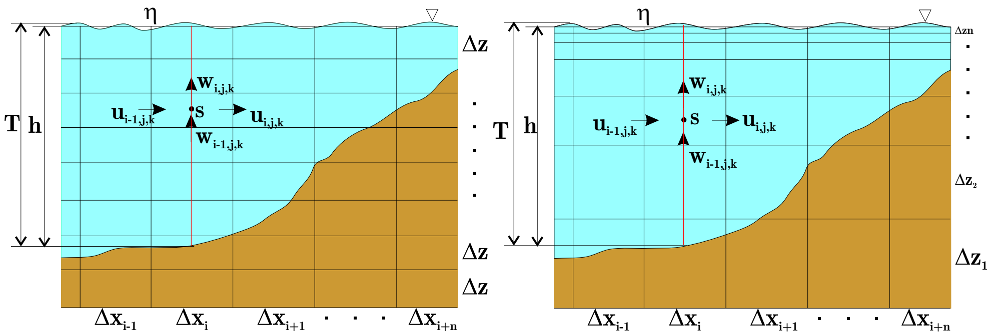

FIGURE 2. Vertical consideration of the YAXUM/3D model: on the left, constant layers; on the right, variables layers

The Eulerian-Lagrangian method separates the equations in two components: advection and diffusion, and each-one is solved by a specific technique. Frequently, the advective components is solved by the characteristic method (Lagrangian). That means that at each node at time t^{n+1} some value is assigned for the particles and this value remains unchanged whereas the particles moves on the characteristic line defined by the flow. The position of this particle in time t^n is localized and by means of an interpolation method between the two adjacent nodes, the new concentration is estimated and assigned to the node at time t^{n+1}. The diffusive component is solved by centered finite differences (Eulerian component) using the concentrations obtained in the previous Lagrangian approach as a initial condition. In this way, advective and diffusive components of the Reynolds and transport equations are solved.

Because the errors are increased with the number of interpolations, as the time step, Δt, is greater, the number of interpolations will decrease so the precision will be improved significatively. This is an advantage regarding the Eulerian methods that their precision diminishes quickly when the Δt is increased.

It can be shown[4] that when a three-lineal interpolation is used, the Eulerian-Lagrangian scheme is free of false oscillations, in addition, it can be shown that the condition of stability is given by

$$\Delta t \leq \left[2\nu_T \left(\frac{1}{\Delta x^2} + \frac{1}{\Delta y^2} \right) \right]^{-1} \tag{9}$$

As we can see, when $\nu_T = 0$, this scheme ends up as unconditionally stable.

2.0.3. Turbulence modeling. In this paper the Reynolds stress correlations $\overline{u'u'}$, $\overline{u'v'}$,$\overline{u'w'}$,. . . ,$\overline{v'w'}$ are modeled by means of zero turbulence model. These correlations are evaluated by a relation of mean velocity gradients related with two turbulent viscosity coefficients ν_{TH} and ν_{TV}. Therefore, the Reynolds stress tensors of equation (2) and (3) have the following form

Velocity U

$$\frac{\partial}{\partial x} \left(2\nu_{TH} \frac{\partial \overline{U}}{\partial x} \right) + \frac{\partial}{\partial y} \left[\nu_{TH} \left(\frac{\partial \overline{U}}{\partial y} + \frac{\partial \overline{V}}{\partial x} \right) \right] + \frac{\partial}{\partial z} \left(\nu_{TV} \frac{\partial \overline{U}}{\partial z} \right) \tag{10}$$

Velocity V

$$\frac{\partial}{\partial y}\left(2\nu_{TH}\frac{\partial \overline{V}}{\partial y}\right)+\frac{\partial}{\partial x}\left[\nu_{TH}\left(\frac{\partial \overline{U}}{\partial y}+\frac{\partial \overline{V}}{\partial x}\right)\right]+\frac{\partial}{\partial z}\left(\nu_{TV}\frac{\partial \overline{V}}{\partial z}\right) \tag{11}$$

where $\nu_{TH}$is calculated in terms of Smagorinsky[7] criterion, as a function of the local horizontal grid resolution (Δx and Δy) and the mean velocity gradients $\overline{U}$ and $\overline{V}$, such that,

$$\nu_{TH}=C_{smag}\Delta x\Delta y\left[\left(\frac{\partial \overline{U}}{\partial x}\right)^2+\frac{1}{2}\left(\frac{\partial \overline{U}}{\partial y}+\frac{\partial \overline{V}}{\partial x}\right)^2+\left(\frac{\partial \overline{V}}{\partial y}\right)^2\right]^{\frac{1}{2}} \tag{12}$$

The vertical mixing is evaluated after the formulation of Stanby[8]:

(13)
$$\nu_{TV}=\left(l_h^4\left[2\left(\frac{\partial \overline{U}}{\partial x}\right)^2+2\left(\frac{\partial \overline{V}}{\partial y}\right)^2+\left(\frac{\partial \overline{V}}{\partial x}+\frac{\partial \overline{U}}{\partial y}\right)^2\right]\right)+l_v^4\left[\left(\frac{\partial \overline{U}}{\partial z}\right)^2+\left(\frac{\partial \overline{V}}{\partial z}\right)^2\right]^{\frac{1}{2}}$$

where l_h is long scale for the horizontal motion and l_v for the vertical motion; both variables are obtained after the following expressions:

$$l_h=\beta l_v, \tag{14}$$

$$l_v=k(z-zb)\text{ for }\frac{(z-z_b)}{\Delta z}<\frac{\lambda}{k},$$

$$l_v=\lambda\Delta z\text{ for }\frac{\lambda}{k}<\frac{(z-z_b)}{\Delta z}<1$$

3. Baroclinic modeling

Equation (1) is written in the following way

$$\overline{P}\left(x,y,z,t\right)=g\int_z^\eta \rho dz+P_{atm} \tag{15}$$

where $\eta=\eta\left(x,y\right)$ is the free surface variation and P_{atm} is the atmospheric pressure. Including equation (15) into (2) and (3) and applying the Leibnitz integration rule, the pressure terms are written as

$$-\frac{1}{\rho_0}\frac{\partial \overline{P}}{\partial x}=-\frac{\rho g}{\rho_0}\frac{\partial \overline{\eta}}{\partial x}-\frac{g}{\rho_0}\int_z^\eta \frac{\partial \rho'}{\partial x}dz-\frac{1}{\rho_0}\frac{\partial P_{atm}}{\partial x} \tag{16}$$

$$-\frac{1}{\rho_0}\frac{\partial \overline{P}}{\partial y}=-\frac{\rho g}{\rho_0}\frac{\partial \overline{\eta}}{\partial y}-\frac{g}{\rho_0}\int_z^\eta \frac{\partial \rho'}{\partial y}dz-\frac{1}{\rho_0}\frac{\partial P_{atm}}{\partial y} \tag{17}$$

where $\rho'=\rho-\rho_0$ is the anomalous density.

So the pressure is related at any depth by the atmospheric pressure P_{atm} acting on the free surface, the variation of the free surface $\overline{\eta}$ (barotropic component) and the anomalous pressure integrated between that depth and the free surface (baroclinic component). Therefore, if the equations (16) and (17) are substituted in the equations (2) and (3), respectively, the equations of the horizontal hydrodynamic field including the baroclinic term is given by,

$$\frac{\partial \overline{U}}{\partial t} + \overline{U}\frac{\partial \overline{U}}{\partial x} + \overline{V}\frac{\partial \overline{U}}{\partial y} + \overline{W}\frac{\partial \overline{U}}{\partial z} = -\frac{\rho g}{\rho_0}\frac{\partial \overline{\eta}}{\partial x} - \frac{g}{\rho_0}\int_z^{\eta}\frac{\partial \rho'}{\partial x}dz - \frac{1}{\rho_0}\frac{\partial P_{atm}}{\partial x} - \frac{\partial \overline{u'u'}}{\partial x} - \frac{\partial \overline{u'v'}}{\partial y} - \frac{\partial \overline{u'w'}}{\partial z} + f\overline{V} \tag{18}$$

$$\frac{\partial \overline{V}}{\partial t} + \overline{U}\frac{\partial \overline{V}}{\partial x} + \overline{V}\frac{\partial \overline{V}}{\partial y} + \overline{W}\frac{\partial \overline{V}}{\partial z} = -\frac{\rho g}{\rho_0}\frac{\partial \overline{\eta}}{\partial y} - \frac{g}{\rho_0}\int_z^{\eta}\frac{\partial \rho'}{\partial y}dz - \frac{1}{\rho_0}\frac{\partial P_{atm}}{\partial y} - \frac{\partial \overline{v'u'}}{\partial x} - \frac{\partial \overline{v'v'}}{\partial y} - \frac{\partial \overline{v'w'}}{\partial z} - f\overline{U} \tag{19}$$

4. Plume dispersion modeling of a fresh water coming into a reservoir

In this part we present a numerical modeling of a thermal fresh water plume dispersion entering into a cold water large reservoir, with uniform depth and infinite length in the direction of the discharge. In Figure 3 is shown the domain and the implemented grid.

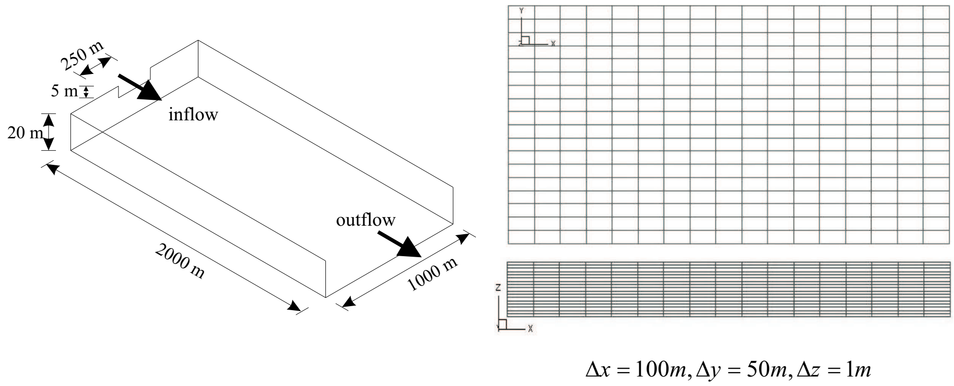

FIGURE 3. Study field and grid generated for the temperature dispersion plume

4.1. Initial conditions. Initially, the velocities and temperatures are setup to zero ($U_E, V_E, W_E = 0 \quad m/s$ and $T_E = 0^oC$). The salinity, wind effect on the surface and Coriolis effect were not considered. At the bottom a constant valor of 1 cm for the rugosity was imposed. For the plume, a constant value of Froude densimetric number of 2.56 was considered according to McGuirk and Rodi[2] and the discharge flow velocity was 0.6 m/s with a temperature of 20 ^{o}C. The results obtained were compared with the numerical work of McGuirk and Rodi[2] and the experimental results of Lal and Rajaratnam[9].

4.2. Results and discusion. In Figure 4 is shown the comparison of the temperature decay derived by McGuirk and Rodi[2], the experimental results of Lal and Rajaratnam[9] and the values computed by the simulation. The results are in agreement. The two numerical calculations are similar but some differences are found compared to the experimental results which can be attributed to the limitation of the tank extension and, therefore, inducing some recirculation. The main difference between the two numerical models is that the McGuirk and Rodi[2] uses a k-ε turbulence model, while in the YAXUM/3D a mixing length scheme was implemented (described previously).

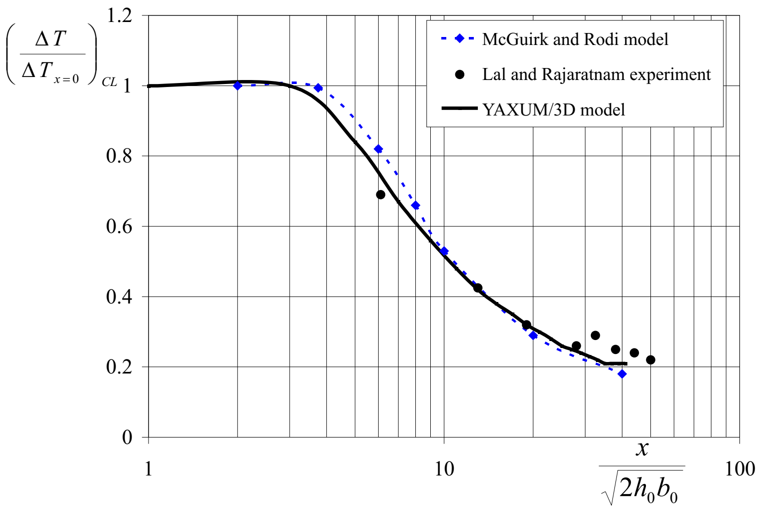

FIGURE 4. Decay temperature comparison. Results of McGuirk and Rodi[2], Lal and Rajaratnam[9], and the YAXUM/3D model are included

In Figure 5(a), it is observed the distribution of the buoyant plume in the vertical plane obtained by McGuirk and Rodi[2]. The behavior of the profile shows a wider plume near the injection which decreases gradually as it moves away. In Figure 5(b), a surface view of the plume is shown. The isotherms correspond to a relationship among the injection temperature and the calculated $(\Delta T/\Delta T_{x=0})$.

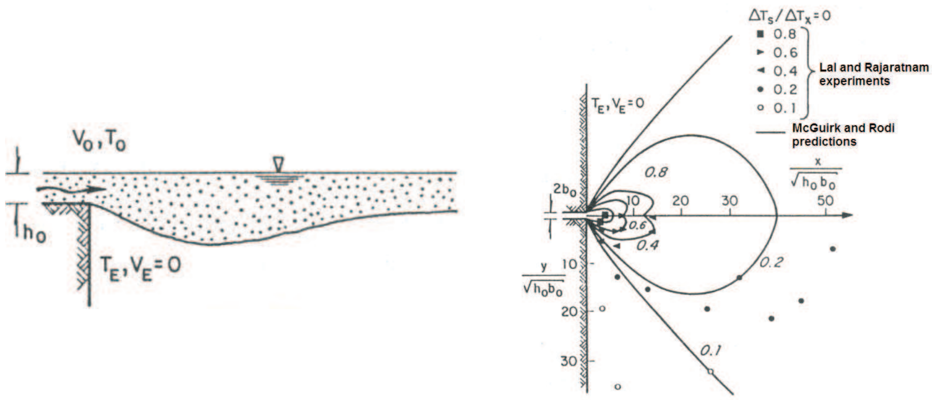

(a) Side view of temperature plume dispersion

(b) Surface isotherms for the temperature plume dispersion (Fr = 2.56)

FIGURE 5. 3-D temperature plume dispersion obtained by McGuirk and Rodi[2] and experimental measurements of Lal and Rajaratnam[9]

In Figure 6 are shown the results of the YAXUM/3D model. The longitudinal section of the plume evolution is described and it can be observed how the plume temperature close the injection and narrows smoothly as the plume moves far from the discharge area similarly to the results of McGuirk and Rodi[2] (Figure 5a). Finally, in Figure 7 the sequence of the horizontal temperature fields are described. The distribution pattern of the buoyant plume is similar to Figure 5(b) given by McGuirk and Rodi[2].

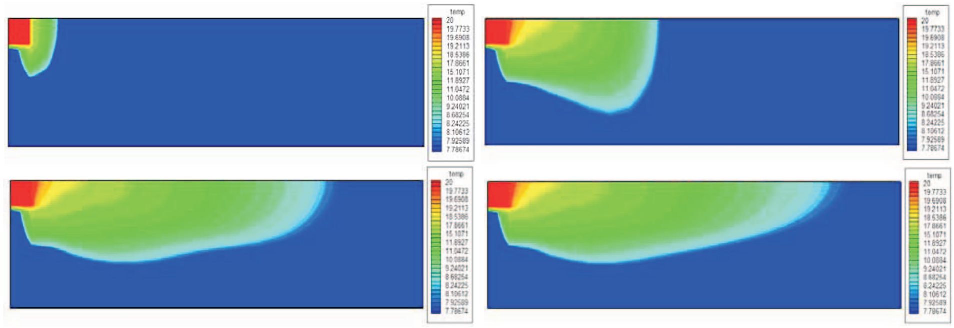

FIGURE 6. Side views of temperature plume dispersion results obtained with the YAXUM/3D model

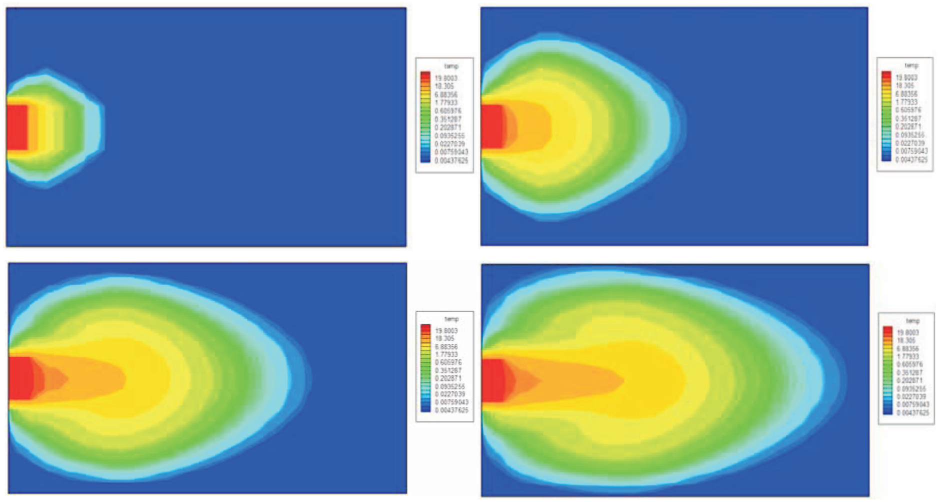

FIGURE 7. Surface views of the temperature plume dispersion evolution obtained with the YAXUM/3D model

4.3. Final comments. The horizontal and vertical patterns of temperatures of the buoyant plume simulated by the YAXUM/3D model are in agreement with the experiments of McGuirk and Rodi[2] and Lal and Rajaratnam[9]. Also, the flotation phenomenon can observed induced by a hot water mass on top interacting with the cold water mass of the reservoir.

5. Plume dispersion modeling of a fresh water discharging to a reservoir: Salinity modeling

The model was also applied to simulate de discharge of low salinity water moving to a reservoir with high salinity concentration like an ocean. The simulations are according to the study carried out by Okely[3] who applied two versions of the ELCOM model for the study of the buoyant plume originated in the discharge of the mouth of the estuary of Leschenault toward the Koombana bay on the West Coast of Australia. The location of the Koombana bay is shown in Figure 8(a) and in Figure 8(b) is shown the characterization of the domain used by Okely[3] which was also implemented for the YAXUM/3D model.

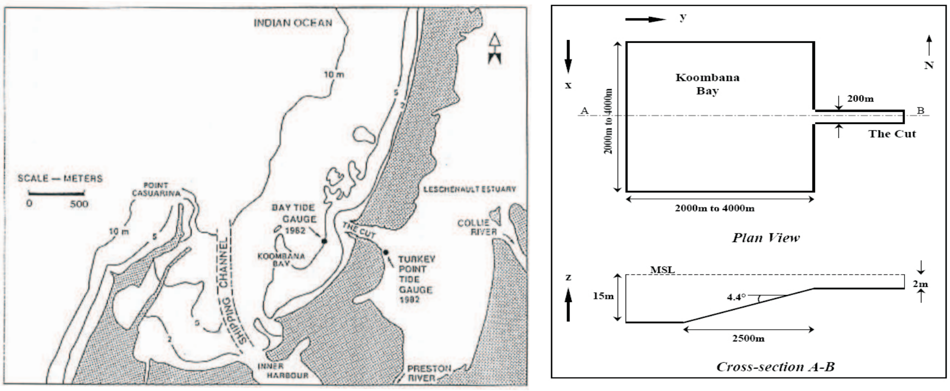

(a) Geographical location (b) Numerical field characterization

FIGURE 8. Study field configuration

5.1. Initial conditions. Initially, the condition of a reservoir is in rest with uniform temperature (16 ^{o}C) and salinity (35 ups) are imposed. The discharge is considered less saline than that of the reservoir with 27 ups and with a lineal increment of the rate flow from 0 m^3/s to 400 m^3/s with a rate of 8.6×10^{-2} m^3/s^2. Other forcings such as Coriolis, wind and variations of temperature were not considered in the simulations. The bottom friction coefficient is 0.05 and constant through the entire domain. These conditions are according to observations carried out by Imberger[10] and Imberger and Luketina[11] during field studies and described described by Okely[3]. The walls of the discharge channel and the reservoir were considered closed in the work of Okely[3]. In contrast, in the simulations with the YAXUM/3D model the wall (face) from the discharge was considered as an open boundary.

5.2. Simulations. Okely[3] modeled the thermal plume dispersion using different grid size resolutions such as 200, 100, 50 and 25 m. In some simulations a variable spacing was applied. The vertical grid size was uniform and was 0.5 m. Two versions of the ELCOM program was used to carry out a total of 11 simulations with time steps of 60, 30 and 20 s, according to the resolution of the grid size..

Simulations with the YAXUM/3D model were made using a constant spacing of 200 m and 25 m (Figure 9) with a vertical grid size of 0.5 m. The time steps were estimated according to the stability of the equation 9.

5.3. Results and discussion. In Figure 10 are shown the results from the ELCOM model, version 1.3.0, using the grid sizes of 200 and 25 m. The salty plume is advected and spreads on the surface and the resolution of the gradients depends on the grid size. For the 200 m grid size the plume is elongated along the x-axis. However, as the grid size is decreased to 25 m the shape of the plume is circular.

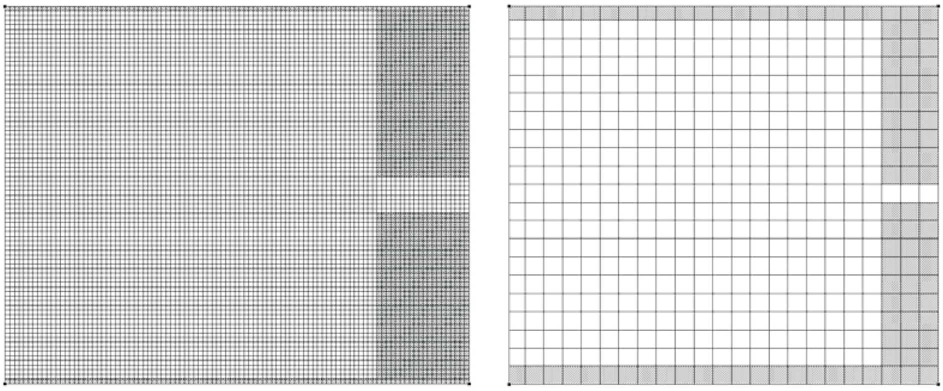

(a) $\Delta x = \Delta y = 25m, \Delta z = 0.5m$ (b) $\Delta x = \Delta y = 200m, \Delta z = 0.5m$

FIGURE 9. Numerical grid implemented on the YAXUM/3D model

Figure 11 shows the surface view of the results of the ELCOM models, version 1.4.2. From these simulations, it was observed that the shape of the saline plume was not dependent on the grid size and behaved similarly under different environmental conditions. This was achieved since the new ELCOM code was significantly improved such as in the grid and interpolations of the variables and velocities.

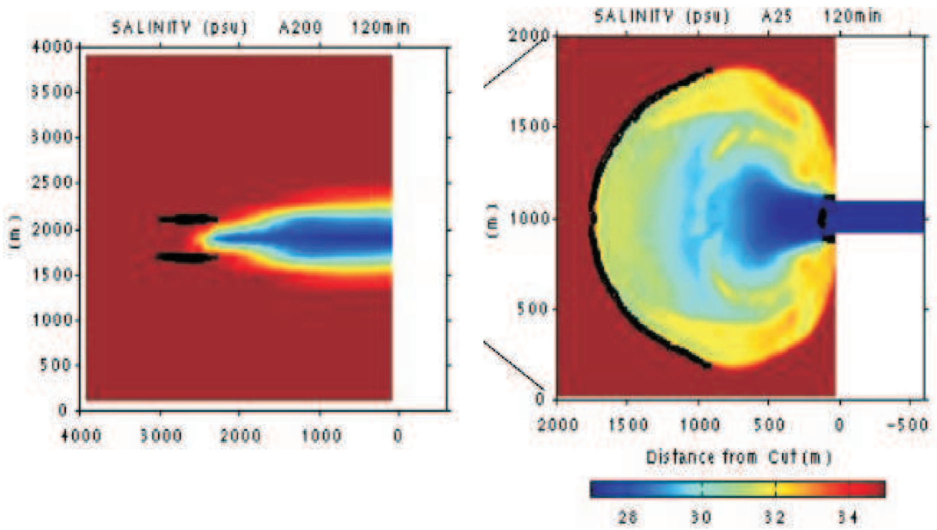

(a) $\Delta x = \Delta y = 200m, \Delta z = 0.5m$ (b) $\Delta x = \Delta y = 25m, \Delta z = 0.5m$

FIGURE 10. Surface buoyant plume obtained with ELCOM 1.3.0 model

A comparison of the results of the YAXUM/3D model and ELCOM (version 1.4.2) shows a slight elongation of the plume along the x-axis and this seems to be to the boundary condition taken in the discharge (Figure 12). However, in both model cases (Figures 12a and b), the plumes tend to be circular as shown in Figures 10(b), 11(a) and 11(b).

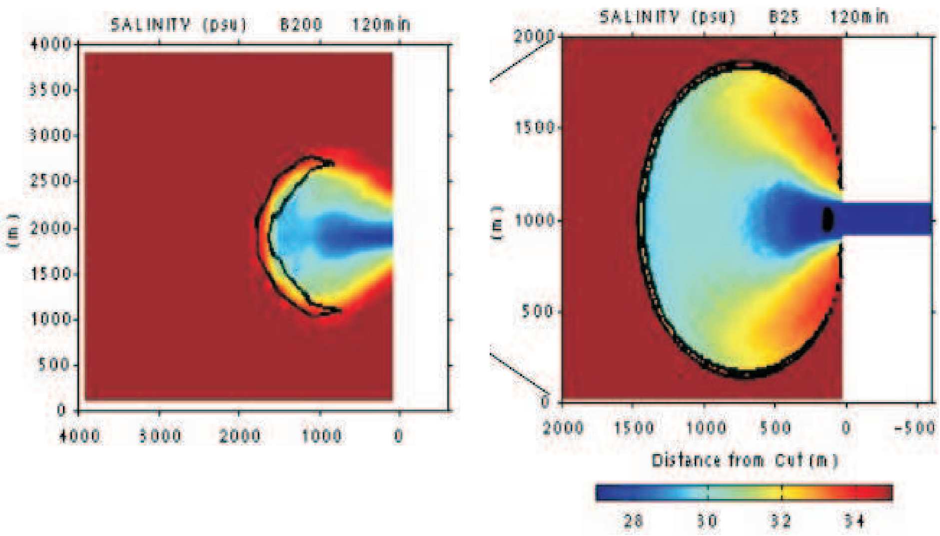

(a) $\Delta x = \Delta y = 200m, \Delta z = 0.5m$ (b) $\Delta x = \Delta y = 25m, \Delta z = 0.5m$

FIGURE 11. Surface buoyant plume obtained with ELCOM 1.4.2 model

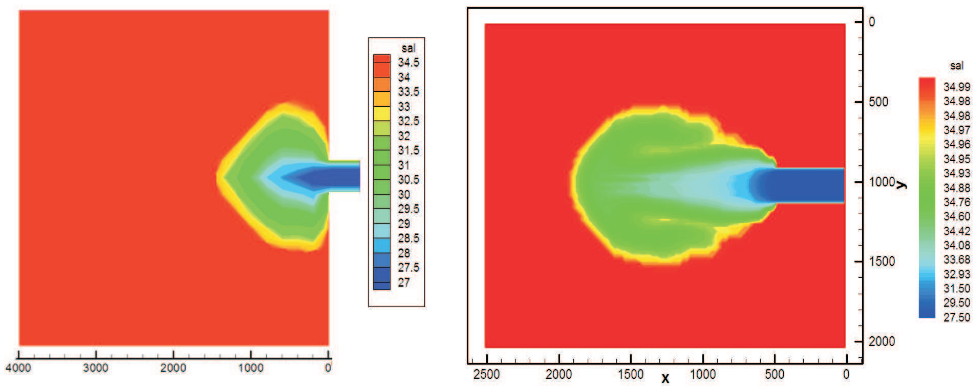

(a) $\Delta x = \Delta y = 200m, \Delta z = 0.5m$ (b) $\Delta x = \Delta y = 25m, \Delta z = 0.5m$

FIGURE 12. Surface buoyant plume obtained with YAXUM/3D model

In relation to vertical structure, in Figure 13(a) and (b) is shown the plume distribution along the x-axis derived form the ELCOM code (version 1.4.2) and that derived by the YAXUM/3D model using, in both cases, a grid resolution of 25 m.

Moreover, Okely[3] also compared the results of the density structure particularly in the *Lift-Off* zone which is the region where the discharge meets the reservoir or bay and the slope of the bay is present. In Figure 14 the field observations made by Imberger and Luketina[11] and the ELCOM and YAXUM/3D model results which are in complete agreement (Figure 14 a, b and c).

Simulations of the vertical salinity distribution with the YAXUM/3D model (Figure 13b) show a slight less stratified vertical structure, as that observed in the

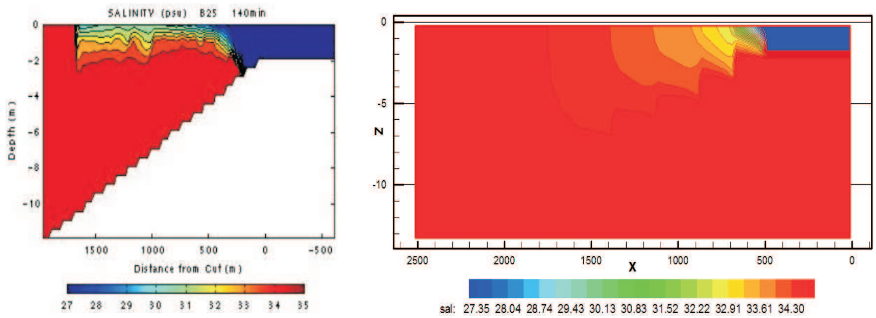

(a) ELCOM 1.4.2. Model (b) YAXUM/3D Model

FIGURE 13. Vertical structure of salinity plume

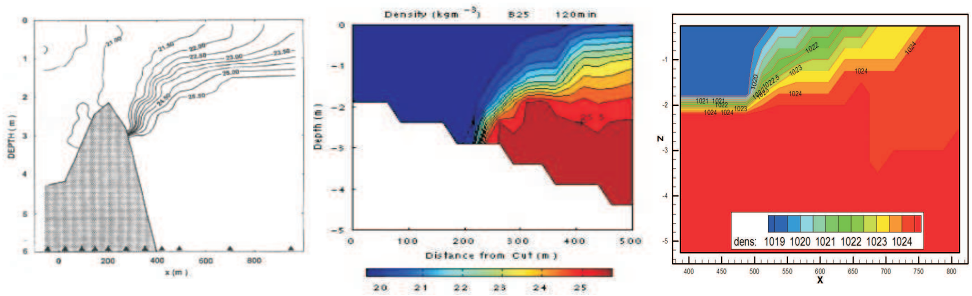

(a) Imberger and Luketina (2001)

(b) ELCOM 1.4.2. Model $\Delta x = \Delta y = 25m, \Delta z = 0.5m$

(c) YAXUM/3D Model $\Delta x = \Delta y = 25m, \Delta z = 0.5m$

FIGURE 14. Density contours comparison on the lift-off region

results of the ELCOM Model (Figure 13a), since the frontal part of the plume tend to mix more efficiently with saline waters of the reservoir. This mixing effect has been also modeled by Morey[12] who simulated the dispersion of the Mississippi river plume to the Gulf of Mexico. For the simulations, the NCOM model was used with a similar scheme as used by the ELCOM and YAXUM/3D model. A view of the vertical saline plume obtained by Morey[12] is shown in Figure 15 where vertical mixing is according to the results modeled by YAXUM/3D for the Koombana Bay.

6. Conclusions

A numerical model has been developed to simulate the freshwater plumes dispersion. The model named YAXUM/3D was validated and simulations of the dispersion of plumes are in agreement with results derived from other models which have been thoroughly tested in different sites.

During the simulations, the time step was the only constraint to achieve good results. Larger time steps caused numerical instabilities; therefore, caution has to be taken to determine the adequate time step and, consequently, achieve realistic results.

Finally, the model constitutes a valuable tool to investigate and quantify the dispersion of freshwater plumes under different environmental conditions. Multiples applications are expected from the model related to the design and evaluation of the impact to the aquatic environment by thermal plumes such as those induced

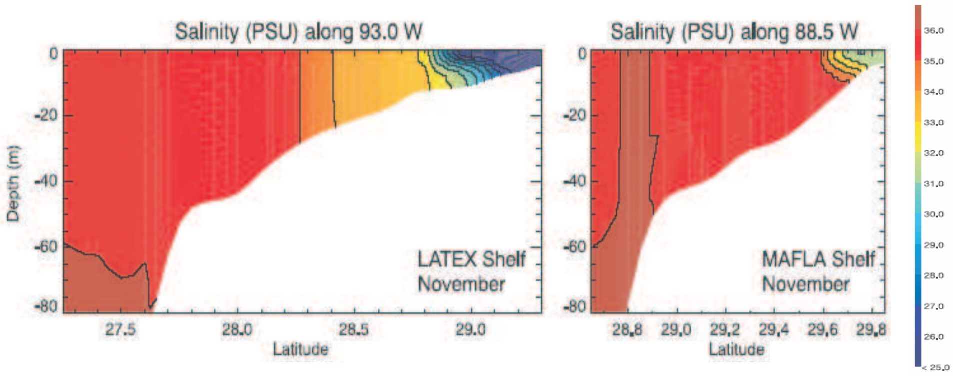

FIGURE 15. Salinity plume vertical distribution of Mississippi river obtained by Morey[12] with NCOM model, on the region of LATEX and Mafla, USA

by power plants along the coast. Now some modules of water quality and sediment transport have been developed; some applications real ecosystems are carried out[13].

Acknowledgments

The authors thank Dr. Ruben Morales Pérez from the Instituto Mexicano de Tecnología del Agua for his comments and technical support during this work.

References

[1] Tait, R.V., Elementos de ecologa marina. Ed. Acubia, 1971.
[2] McGuirk, J. J., and Rodi, W., Numerical model for heated three-dimensional jets, in Heat Transfer and Turbulent Bouyant Convection, Studies and applications for Nat Envir, Buil, Eng Systems. Ed. by Spalding, D. B. and Afgan, N., Hemisphere Publishing Corp. EUA., 1977.
[3] Okely, P., Numerical modelling of bouyant surface discharge characteristics in Koombna bay. The University of Western Australia, Department of Environmental Engineering, Australia, 2001.
[4] Casulli, V., and Cheng, R. T., Semi-implicit finite difference methods for three dimentional shallow water flow. International Journal for numerical methods in fluids, Volume 15, pp. 629-648, 1992.
[5] UNESCO, Tenth report of the joint panel on oceanographic tables and standards. UNESCO Tech. Papers in Marine Sci. No 36, Paris, 1981.
[6] UNESCO, Background papers and supporting data on the International Equation of State of seawater 1980. UNESCO technical papers in marine science, 38, 192 pp., 1981.
[7] Smagorinsky, J., General circulation experiments with the primitive equations. 1. Basic experiment, Mon. Weather Rev., 91, 99-164, 1963.
[8] Stansby, P. K., A mixing-length model for shallow turbulent wakes. J. Fluid Mech., vol. 495, pp. 369-384, Cambridge University Press., United Kingdom, 2003.
[9] Lal, P. B. B. and Rajaratnam, N., An experimental study of heated surface discharges into quiescent ambient. Dept. of Civil Eng., Alberta University, Canada. 1976.
[10] Imberger, J., Tidal Jet Frontogenesis, Mech. Eng. Trans. Inst. Eng. Aust., vol.8, pp. 171-180. 1983.
[11] Imberger, J., and Luketina, D.,Turbulent motions in a surface buoyant jet, in Proceedings of the Third International Symposium on Stratified Flows, eds. E.J. List and G.H. Jirka, Pasadena, pp. 755-771. 1988.
[12] Morey, S. L., Martin, P. J., O'Brien, J. J., Wallcraft, A. A., and Zavala, H. J., Export pathways for river discharged fresh water in the northern Gulf of Mexico. Journal of Geophysical Research, Vol. 108, No. C10, 3303, 15p, 2003.

[13] Ramrez, H., Rodriguez, C., and Herrera, E. Multilayer hydrodynamic model and their application to sediment transport in estuaries, Currents trends in High performance Computing and its applications Proceedings of the international Conference on High Performance Computing and Applications. Springer Verlag, XXXI, 639 p. ISBN 3-540-25785-3

Instituto Mexicano del Petróleo, Eje Central Lázaro Cárdenas 152, San Bartolo Atepehuacan. CP. 07730, México D.F., México
E-mail: `hrleon@imp.mx`
URL: `http://www.imp.mx`

Escuela Superior de Ingeniería y Arquitectura, Unidad Zacatenco, Instituto Politécnico Nacional, México D.F., México
E-mail: `bphhector@yahoo.com`
URL: `http://www.ipn.mx`

Universitè Aix-Marseille III. Marseille, France
E-mail: `cuevas@L3m.univ-mrs.fr`
URL: `http://www.L3m.univ-mrs.fr`

Instituto Mexicano del Petróleo, Eje Central Lázaro Cárdenas 152, San Bartolo Atepehuacan. CP. 07730, México D.F., México
E-mail: `ccouder@imp.mx`
URL: `http://www.imp.mx`